Analytical and Experimental Investigations of Laminar Mixing of Confined Heterogeneous Jets

GIDEON SHAVIT*
Honeywell Inc., Arlington Heights, Ill.
AND
ZALMAN LAVAN†
Illinois Institute of Technology, Chicago, Ill.

This study is concerned with the mixing process in the initial region of coaxial laminar jets. The Navier-Stokes equations were solved numerically using vorticity, stream function, and concentration with variable properties. Then, the pressure is calculated from the known velocity field. Experimental investigations were conducted in coaxial tubes with radius ratio of 0.25 and mixing length of 30 in. The validity of the numerical results and regions of laminar flow were established for air-air and air-argon jets. The presence of recirculating cells and the influence of the entrance conditions on the mixing process were analyzed. It was found that the fully developed entrance velocity profiles and low-density ratio enhance the formation of cells. The fully developed entrance velocity profiles demonstrate pressure rise in the near mixing region due to augmentation while the plug-shaped entrance profiles demonstrate immediate pressure loss.

Nomenclature

A = cross section area
a = constant defined in Eq. (11)
B = constant defined in Eq. (12)
C_2 = concentration of the outer specie
D = pipe diam
D_{kl} = diffusion coefficient between the kth and the lth component
$f_1(r).f_2(r)$ = shape of entrance velocity profiles
H = tangential vorticity divided by radial distance, $H = \eta/r$
JM = number of grid points in the upstream section
M_k = molecular weight of the kth component
N_k, M_k = coefficients defined in Eq. (13)
P = pressure
R = radius of tube
R_e = Reynolds number based on the diam and average velocity and reference viscosity
$\bar{R}_e$ = $\psi_m/R_2 = R_e/4$
Re_j = Reynolds number of inner jet
r = radial coordinate
S_c = Schmidt number, defined in Eq. (5)
T = temperature
V_j = inner jet velocity
V_0 = outer jet velocity
u, w = radial and axial velocities in a cylindrical coordinate system
$\bar{w}$ = average velocity of the mixture
x_k = mole fraction of the kth component
x = axial distance in the transformed plane
z_0 = location of upstream boundary conditions
z = axial coordinate
z_{max} = value of z at second-to-the-last grid point
α = coefficient defined in Eq. (11)
η = tangential vorticity component
μ = coefficient of dynamic viscosity
ν = kinematic coefficient of viscosity μ/ρ
ρ = density
ρ_j = inner jet density
ρ_0 = outer jet density
ψ = stream function

Subscripts
p = pure gas
1 = refer to inner jet
2 = refer to outer jet

Superscript
* = dimensional quantity

Presented as Paper 71-601 at AIAA 4th Fluid and Plasma Dynamics Conference, June 21–23, 1971, Palo Alto, Calif.; submitted March 2, 1972; revision received October 2, 1972. This investigation was supported by NASA Grant NSG-694.

Index categories: Nozzle and Channel Flow; Viscous Nonboundary-Layer Flows; Nuclear Propulsion.

* Senior Staff Analyst. Member AIAA.

† Associate Professor, Mechanical Engineering Department. Member AIAA.

Introduction

THE problem of heterogeneous coaxial jet mixing in a confining tube is investigated. At sufficiently large velocity ratios, recirculation regions are often present; hence, the boundary-layer equations are in general invalid. In the present investigation, the steady Navier-Stokes equations with variable properties are solved numerically and the solutions are compared with experimental results.

In 1949, von Kármán[1] showed, by means of an inviscid model, the importance of the velocity profile in the entrance to the mixing region of confined jets. Weinstein and Todd[2] solved the problem of mixing in unconfined laminar coaxial streams of greatly different densities. This analysis is based on boundary-layer assumptions with constant pressure in the entire flowfield. The problem was solved numerically in the von Mises plane.

The first extensive experimental study was conducted by Wood[3] in 1964, who showed that under certain conditions, the flow in the mixing region remains laminar. Seider and Churchill[4] in 1968 solved the problem of confined jet mixing with chemical reaction, assuming the velocity profile at the entrance to be fully developed. They solved the problem numerically using an implicit alternating-direction scheme, with the assumption that temperature and mixture properties remain

constant, thus decoupling the diffusion and energy equations from the rest of the system. Their results compared relatively well with Wood's[3] data for equimolar diffusion.

Ghia et al.[5] applied the approach suggested by Weinstein and Todd[2] for confined jet mixing. They introduced a confining wall, thus taking into account axial pressure gradients.

Definition of the Problem

The mathematical model consists of two laminar jets coflowing at different velocities in coaxial tubes. At a given point ($z = 0$) the inner tube terminates and the mixing process begins.

The analytical problem is divided into two cases: I) The inner and outer jets have fully developed velocity profiles at a given station z_0, upstream of the entrance to the mixing region (see Fig. 1). II) The velocity profiles of the inner and the outer jets are prescribed at the entrance to the mixing region, $z = 0$. Case I is a more realistic statement of the jet mixing problem, since it allows an upstream influence.

The objective of this investigation is to gain a better understanding of the mechanisms that govern the mixing of confined heterogeneous jets in coaxial tubes. Of particular interest are the cases of large density and velocity ratios, with the inner jet being the heavier and the slower. The presence of recirculating cells, the effects of entrance conditions, and the effect of the parameters governing the flow in the mixing process are studied.

Assumptions and Governing Equations

The equations that govern the flow of a binary fluid mixture are: the conservation of mass, momentum, and energy, and the equation of mass diffusion. In the present analysis it is assumed that there are no sources of mass and energy; there are no body forces; mixing is isothermal; diffusion is only due to concentration gradient; and the mixture is ideal and incompressible. With these simplifications all physical properties are expressed as a function of concentration only and the energy equation is decoupled from the system. The dimensionless form of the governing equations for steady axisymmetric laminar incompressible flow in terms of stream function, vorticity, and concentration are

$$\frac{\partial^2\psi}{\partial z^2}+\frac{\partial^2\psi}{\partial r^2}-\frac{1}{r}\frac{\partial\psi}{\partial r}-\frac{1}{\rho}\frac{\partial\rho}{\partial r}\frac{\partial\psi}{\partial r}-\frac{1}{\rho}\frac{\partial\rho}{\partial z}\frac{\partial\psi}{\partial z}=r^2\rho H \tag{1}$$

$$\frac{\partial^2 H}{\partial z^2}+\frac{\partial^2 H}{\partial r^2}+\frac{3}{r}\frac{\partial H}{\partial r}-\frac{\bar{R}_e\rho}{\mu}\left[u\left(\frac{\partial H}{\partial r}+\frac{H}{r}\right)+w\frac{\partial H}{\partial z}+H\frac{\partial u}{\partial r}+\frac{\partial w}{\partial z}\right]+\frac{2}{\mu}\frac{\partial\mu}{\partial z}\left[\frac{\partial H}{\partial z}-\frac{1}{r}\frac{\partial}{\partial r}\left(\frac{u}{\rho}\frac{\partial\rho}{\partial r}+\frac{w}{\rho}\frac{\partial\rho}{\partial z}\right)\right]+\frac{2}{\mu}\frac{\partial\mu}{\partial r}\left[\frac{\partial H}{\partial r}+\frac{3}{2}\frac{H}{r}+\frac{1}{r}\frac{\partial}{\partial z}\left(\frac{u}{\rho}\frac{\partial\rho}{\partial r}+\frac{w}{\rho}\frac{\partial\rho}{\partial z}\right)\right]+\frac{\bar{R}_e}{\mu r}\left[\frac{\partial\rho}{\partial r}\left(u\frac{\partial w}{\partial r}+w\frac{\partial w}{\partial z}\right)-\frac{\partial\rho}{\partial z}\left(u\frac{\partial u}{\partial r}+w\frac{\partial u}{\partial z}\right)\right]+\frac{2}{\mu r}\frac{\partial^2\mu}{\partial r\partial z}\left(\frac{\partial u}{\partial r}-\frac{\partial w}{\partial r}\right)+\frac{1}{\mu r}\left(\frac{\partial^2\mu}{\partial z^2}-\frac{\partial^2\mu}{\partial r^2}\right)\left(\frac{\partial u}{\partial z}+\frac{\partial w}{\partial r}\right)=0 \tag{2}$$

$$\frac{\partial^2 C_2}{\partial z^2}+\frac{\partial^2 C_2}{\partial r^2}+\frac{1}{r}\frac{\partial C_2}{\partial r}-\bar{R}_e S_c\left[u\frac{\partial C_2}{\partial r}+w\frac{\partial C_2}{\partial z}\right]+\frac{1}{\rho}\left[\frac{\partial\rho}{\partial r}\frac{\partial C_2}{\partial r}+\frac{\partial\rho}{\partial z}\frac{\partial C_2}{\partial z}\right]=0 \tag{3}$$

where u and w are the radial and axial velocity components defined by

$$u=-\frac{1}{\rho r}\frac{\partial\psi}{\partial z},\quad w=\frac{1}{\rho r}\frac{\partial\psi}{\partial r} \tag{4}$$

and $H = \eta/r$, where η is the tangential component of vorticity.

The equations were made dimensionless using the radius of the outer pipe R_2, the total mass flow rate, ψ_m, and the density and viscosity of the unmixed outer stream as reference quantities. Two nondimensional groups are recognized as:

Reynolds Number

$$\bar{R}_e=\psi_m{}^*/\mu_{p,2}{}^*R_2{}^*=\bar{w}{}^*R_2{}^*\rho_{p,2}{}^*/2\mu_{p,2}{}^*=R_e/4$$

Schmidt's Number

$$S_c=\nu_{p,2}{}^*/D_{12}{}^* \tag{5}$$

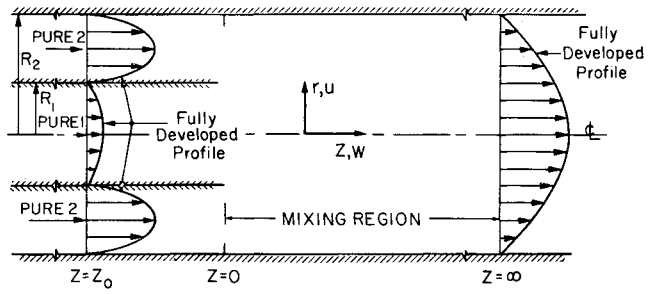

Fig. 1 Confined jet mixing, case I.

Mixture Properties

In keeping with the assumptions above, the density[6] is a function of concentration alone

$$\rho=1\Big/\left[\frac{\rho_{p,2}{}^*}{\rho_{p,1}{}^*}+C_2\left(1-\frac{\rho_{p,2}{}^*}{\rho_{p,1}{}^*}\right)\right] \tag{6}$$

The viscosity is also a function of concentration only. A rather simple equation which has been applied to a wide range of experimental data was derived by Ruddenberg and Wilkie[7] and has the following form:

$$\mu=\frac{\mu_{p,1}{}^*/\mu_{p,2}{}^*}{1+1.385S_{c_1}x_2/x_1}+\frac{1}{1+1.385S_{c_2}x_1/x_2} \tag{7}$$

The diffusion coefficient[8] is considered to be a constant throughout the mixture and is calculated from the Lennard-Jones relation for the potential function[9]:

$$D_{k,l}=0.001858T^{3/2}\frac{[(M_l+M_k)/M_lM_k]^{1/2}}{\sigma_{k,l}{}^2\Omega_D p}\qquad k\neq l,\quad k=1,2,\quad l=1,2 \tag{8}$$

where T = absolute temperature, °K; σ = Lennard-Jones free constant for the mixture, °A; and Ω_D = collision integral.

Pressure Calculation

The pressure is calculated by integrating the axial pressure gradient along the center line, and then integrating the radial pressure gradient from the center line to the wall;

$$\frac{\partial p}{\partial r}=\frac{1}{\bar{R}_e}\left\{\frac{\partial\mu}{\partial r}\left(2\frac{\partial u}{\partial r}-\tfrac{2}{3}\nabla\cdot\bar{V}\right)+\frac{\partial\mu}{\partial z}\left(2\frac{\partial u}{\partial z}-Hr\right)+\mu\left[\tfrac{4}{3}\frac{\partial}{\partial r}(\nabla\cdot\bar{V})+r\frac{\partial H}{\partial z}\right]\right\}-\frac{\rho}{2}\frac{\partial}{\partial r}(u^2+w^2)-\rho wHr \tag{9}$$

$$\frac{\partial p}{\partial z}=\frac{1}{\bar{R}_e}\left\{\frac{\partial\mu}{\partial z}\left(2\frac{\partial w}{\partial r}-\tfrac{2}{3}\nabla\cdot\bar{V}\right)+\frac{\partial\mu}{\partial r}\left(2\frac{\partial w}{\partial z}-Hr\right)+\mu\left[\tfrac{4}{3}\frac{\partial}{\partial r}(\nabla\cdot\bar{V})-\frac{1}{r}\frac{\partial}{\partial r}(r^2H)\right]\right\}-\frac{\rho}{2}\frac{\partial}{\partial z}(u^2+w^2)+\rho uHr \tag{10}$$

Boundary Conditions

The centerline $z_0 \leqq z < \infty$, is a line of symmetry; hence

$$\psi(0,z)=0,\quad(\partial H/\partial r)_{0,z}=0,\quad(\partial C_2/\partial r)_{0,z}=0$$

At the exit, $0 \leqq r \leqq 1$; far downstream the flow is fully developed and completely mixed. Hence

$$(\partial\psi/\partial z)_{r,\infty} = 0, \quad (\partial H/\partial z)_{r,\infty} = 0, \quad (\partial C_2/\partial r)_{r,\infty} = 0$$

Along the outer wall, $z_0 \leqq z < \infty$, the no-slip and no-mass-transfer condition gives

$$\psi(1,z) = 1.0, \quad (\partial C_2/\partial r)_{1,z} = 0, \quad H(1,z) = -(1/\rho)(\partial^2\psi/\partial r^2)$$
$$\text{subjected to} \quad (\partial\psi/\partial r)_{1,z} = 0$$

Along the inner wall, $z_0 \leqq z \leqq 0$,

$$\psi_1(R_1,z) = \int_0^{R_1} (\rho_{p,1}{}^*/\rho_{p,2}{}^*) f_1(r) r dr, \quad \frac{\partial C_2}{\partial r}(R_1,z) = 0,$$

$$H(R_1,z) = -\frac{1}{\rho r^2}\frac{\partial^2\psi}{\partial r^2} \quad \text{subjected to} \quad \frac{\partial\psi}{\partial r}(R_1,z) = 0$$

It should be pointed out that $H(R_1,z)$ is double valued over this length; one value is associated with the inner region and the other with the outer region.

Two types of entrance conditions are used. In the first case, I, fully developed profiles are placed a few radii upstream from the termination point of the inner tube. In the second case, II, entrance profiles are placed at the end of the inner tube. If z_0 is the upstream location at which conditions are specified we have the following:

For $0 \leqq r \leqq R_1$

$$\psi_1(r,z_0) = \int_0^r (\rho_{p,1}{}^*/\rho_{p,2}{}^*) f_1(r) r dr, \quad C_2(r,z_0) = 0,$$

$$H(r,z_0) = -\frac{1}{\rho r^2}\left[\frac{\partial^2\psi}{\partial z^2} + \frac{\partial^2\psi}{\partial r^2} - \frac{1}{r}\frac{\partial\psi}{\partial r}\right]$$

$$\text{subjected to} \quad \frac{\partial\psi}{\partial z}(r,z_0) = 0$$

and for $R_1 \leqq r \leqq 1$

$$\psi_2(r,z_0) = \int_{R_1}^1 f_2(r) r dr, \quad C_2(r,z_0) = 1.0,$$

$$H(r,z_0) = -\frac{1}{\rho r^2}\left[\frac{\partial^2\psi}{\partial z^2} + \frac{\partial^2\psi}{\partial r^2} - \frac{1}{r}\frac{\partial\psi}{\partial r}\right]$$

$$\text{subjected to} \quad \frac{\partial\psi}{\partial z}(r,z_0) = 0$$

Transformation of Coordinates

A transformation of coordinates is used to map the semi-infinite z domain into a finite x domain. In addition, the transformation facilitates the study of rapid change in the flow near the entrance to the mixing region. Two types of transformations are used. The transformation for Case I is

$$x = a + \frac{2}{\pi}(1-a)\tan^{-1}\left[\frac{z}{z_0}\tan\left(-\frac{a}{1-a}\frac{\pi}{2}\right)\right] \tag{11}$$

The constant a is determined by the number of grid points, JM, assigned in the region $z_0 \leqq z \leqq 0$. Since $z = 0$ is located between two grid points, a is defined as follows:

$$a = 0.5[x(JM) + x(JM+1)]$$

This function maps $z_0 \leqq z \leqq \infty$ into $0 \leqq x \leqq 1$. The transformation for Case II is

$$x = z/(z+B) \tag{12}$$

where $B = z_{\max}\Delta x/(1-\Delta x)$, and $z_{\max}$ is the value of z at the last-but-one grid point. This function maps $0 \leqq z \leqq \infty$ into $0 \leqq x \leqq 1$.

Method of Solution

All the governing equations are written in the following form:

$$\left[\left(\frac{dx}{dz}\right)^2\frac{\partial^2}{\partial x^2} + \frac{\partial^2}{\partial r^2} - M_k\frac{\partial}{\partial x} - N_k\frac{\partial}{\partial r}\right]F_k + S_k = 0, \qquad k = 1,2,3 \tag{13}$$

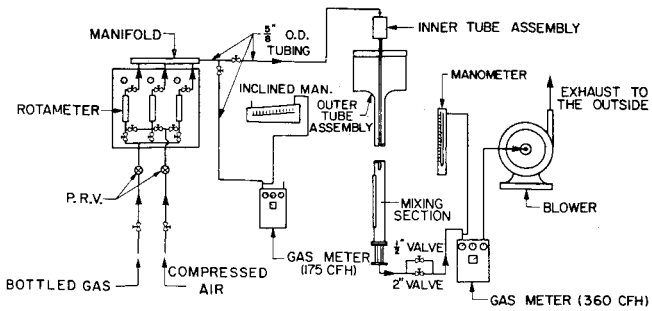

Fig. 2 Schematic layout of experimental flow circuit.

where F_k is the particular variable, S_k represents source terms, and M_k and N_k are the corresponding coefficients.

The equations are replaced by finite-difference approximations. Three point central differences are used in the stream function equation while in the vorticity and in the mass diffusion equations central differences are used for second-order derivatives and upwind differencing for the first-order derivatives. Initial values of ψ, H, and C_2 are first assigned to all grid points, and the corresponding equations are solved by successive overrelaxations, alternately sweeping once with each equation. The relaxation procedure is stopped when the residues decrease below some small preassigned values (typically 10^{-6}). Once the velocity field is obtained, the pressure is calculated from Eqs. (9) and (10). Typically a grid of 21×29 points is used, and execution time on a Univac 1108 is approximately ten minutes. A detailed discussion of the differencing scheme, the numerical procedure, and the stability analysis is given in Refs. 6 and 10.

Experimental Investigation

Description of the Apparatus

The experimental investigation is conducted in coaxial tubes of radius ratio 0.25 ($R_1 = 0.5$ in. and $R_2 = 2$ in.) and a mixing length of 30 in. Compressed air or argon is blown through the inner tube assembly into the mixing section and ambient air is drawn through the outer tube by a blower located downstream of the mixing section. A schematic layout of the experimental flow circuit is shown in Fig. 2. The inner jet enters the inner tube through a plenum chamber which contains straighteners.

The inner jet tube is 0.997 ± 0.002 in. i.d. and 1.125 in. ± 0.002 in. o.d. The tube is 67 in. long, and is made of stainless steel. The inner side is honed and the outer side is hand polished. The downstream end is tapered from the outside to reduce the wall thickness at the exit to 0.008 ± 0.001 in.

The outer tube is supplied with ambient air drawn by the blower which is located downstream. The ambient air passes through a plenum chamber, a contraction section, the outer jet tube, and an outlet section. It enters the plenum chamber through a filter and straighteners. The contraction section provides a uniform velocity profile and separation-free flow at the entrance to the annulus. The outer tube is made from Plexiglass, has an i.d. of 3.950 ± 0.010 in. and an o.d. of 4.460 in., and is 73 in. long.

The inner tube assembly is suspended from supporting rods in the plenum chamber. The downstream end is about 60 in. below the support, and is supported by three needles made from 0.028 in. diam hypodermic tubing. The Reynolds number based on the needle diameter and the air velocity of 1.8 ft/sec is 25.6. Since the needles are 294 needle diameters upstream of the initial mixing region, their presence should not affect the development of the flow in the annular pipe.

The mixed fluids leave the mixing region through an outlet section and enter the flow control mechanism. From there the fluid enters a gas meter which was calibrated at full range and at

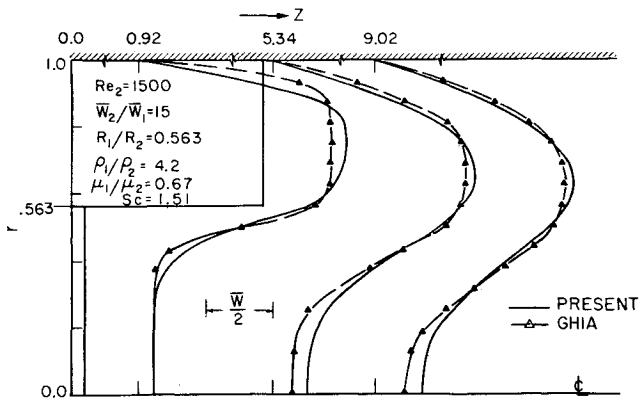

Fig. 3 Comparison of velocity profiles.

25% capacity to an accuracy of 0.8%. The mixture leaves the gas meter, enters the blower and is discharged to the outside.

The experimental program is divided into three main parts, which are: establishment of laminar flow regime, velocity measurements, and concentration measurements.

Instrumentation

Hot wire anemometry is used for velocity measurements in the case of air-air mixing and for establishing the region of inner and outer velocities at which the mixing of coaxial jets in the confined tube remains laminar. The hot-wire anemometer was calibrated in two different calibration tunnels. The first consists of a horizontal 2-in. diam standard pipe, 180 in. long. The second consists of the inner tube assembly, which is positioned vertically and has a uniform velocity profile at the entrance. Comparison of the two calibration curves show a discrepancy of 1% in slope.

Aspirating Probe

The concentration measurements are done with an aspirating probe. A vacuum pump sucks the gas mixture through the opening of the probe, past a hot film and through a hole of 0.008 ± 0.001 in. in a jewel bearing. The capacity of the vacuum pump is large enough to insure sonic velocity at the throat of the bearing. The sonic velocity is a function of the gas constant, molecular weight, specific heat ratio, and temperature of the mixture. For an isothermal gas mixture the sonic velocity is the function of concentration only.

The aspirating probe is calibrated in the apparatus. A mixture with known composition is prepared and blown through the inner tube assembly. For each mixture composition the output of the probe is recorded, thus establishing a calibration curve which is updated each time data is taken.

The hot-wire probe and the aspirating probe are mounted on a traverse mechanism. This arrangement allows axial and radial movement of the probe throughout the mixing region.

Results and Discussion

Analytical Results

The validity and accuracy of the present numerical procedure was in part established by comparing computed results with known solutions and with experimental data. The flow development in a circular pipe was calculated first. Agreement with known results is very good. The second comparison is with the experimental data of Wood[3] who measured the concentration field for the case of mixing of equimolar jets. The agreement of the computed results with the experimental data is also very good. The last comparison deals with mixing of heterogeneous jets (density ratio 4.2). The present results are compared with calculated values of Ghia et al.[5] who solved the boundary layer equations. The results shown in Fig. 3, deviate only in the initial part of the mixing region, where the radial velocity is important.

Following these comparison the influence of the various parameters on jet mixing was studied in detail. The Reynolds number is varied from zero to 2000, the radius ratio from 0.3 to 0.7, the velocity ratio from 0.05 to 100,000, the density ratio from 1 to 8.3, viscosity from 0.67 to 1, and Schmidt number from 0.76 to 2.02. For certain combinations for parameters, recirculation cells are formed near the tube wall when the inner flow is faster, and near the axis when the outer flow is faster. In the following discussion (with the exception of Fig. 9) results are presented only for the case of a fast and light outer stream, and a slow and heavy inner stream. Figure 4 shows that for given conditions cell formation takes place at high velocity ratios (strong shear layer). As the velocity ratio increases (all other parameters being held constant), the cell grows in the upstream direction while its downstream end hardly moves. For an infinite velocity ratio, the cell propagates upstream and extends into the whole region of the inner tube.

The influence of the density ratio on cell formation is shown in Fig. 5. The heavier the inner jet (for the same velocity ratio), the smaller the influence of the outer jet on the inner

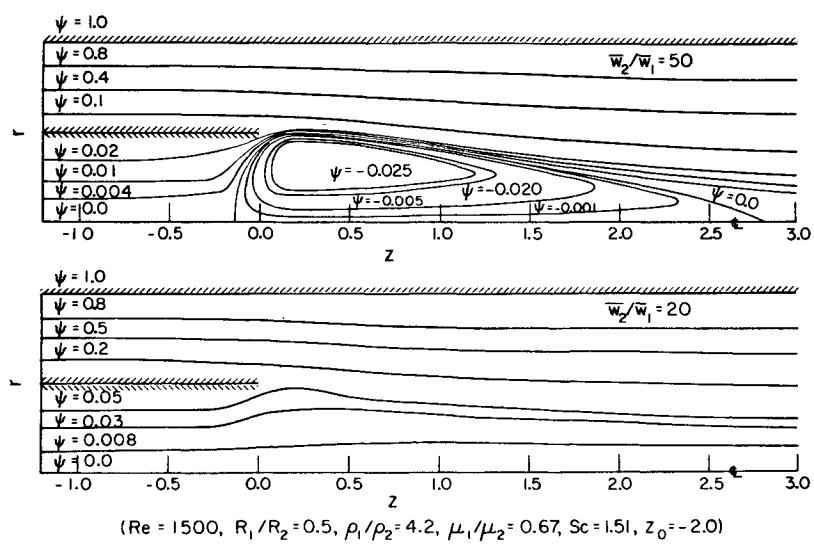

Fig. 4 Streamline contours, variable velocity.

(Re = 1500, R_1/R_2 = 0.5, ρ_1/ρ_2 = 4.2, μ_1/μ_2 = 0.67, Sc = 1.51, Z_0 = -2.0)

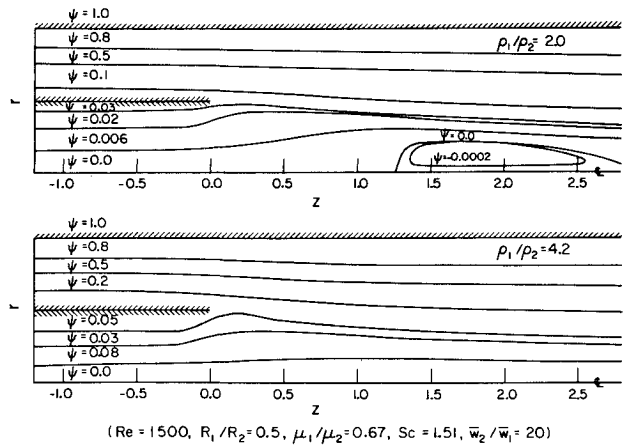

(Re = 1500, $R_1/R_2 = 0.5$, $\mu_1/\mu_2 = 0.67$, Sc = 1.51, $\bar{w}_2/\bar{w}_1 = 20$)

Fig. 5 Streamline contours, variable density.

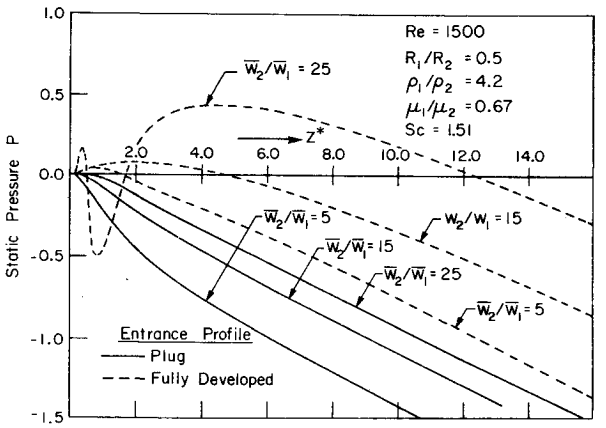

Fig. 7 Pressure development along centerline.

stream flow development. This is clearly due to the larger inner jet momentum. Cell formation also depends on the entrance velocity profile to the mixing region. Fully developed profiles, placed at the entrance to the mixing region, generate recirculating cells at lower velocity ratios than plug profiles. The fully developed profiles prescribed upstream of the entrance to the mixing region generate cells at velocity ratios that are intermediate to those required by plug and fully developed entrance profiles. The latter case is the most realistic since the upstream influence cannot be neglected when the velocity ratio is large.

The effect of the shape of the velocity profile in the entrance to the mixing region on the mixing process and the required developing length is shown in Fig. 6. For velocity ratio of unity, the center line velocity of the fully developed profile hardly changes; whereas, for plug entrance profile the flow accelerates to twice the value at the entrance section. For a velocity ratio of five, the fully developed profile retards locally near the entrance; whereas in the case of the plug profile the flow continuously accelerates. At a velocity ratio of twenty, the fully developed profile retards considerably, while the plug profile retards only in the very near region.

The pressure distribution along the centerline for plug and fully developed entrance profiles is shown in Fig. 7 as a function of velocity ratio. Plug profiles provide favorable pressure gradients up to velocity ratios of 25 while fully developed profiles yield adverse pressure gradients in the near mixing region already at a velocity ratio of five. Far downstream the pressure gradient in both cases is favorable due to the friction at the wall.

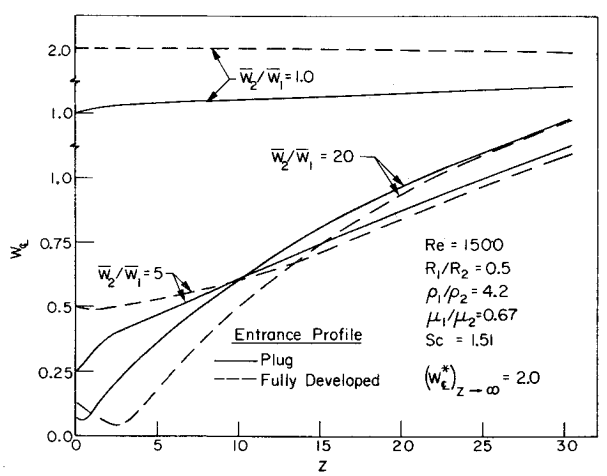

Fig. 6 Velocity development along centerline.

The different behavior of the plug and fully developed profiles is due to the early influence of the wall on the flow development. For plug profile the flow retards near the wall, thus tending to cause an acceleration of the fluid in the interior and therefore a favorable pressure drop. The effect of the mixing layer is similar for the two entrance profiles. The flow locally accelerates, tending to reduce the center line velocity, and to increase the pressure. At high velocity ratios the relative effect of the shear layer dominates, the flow retards at the center line and recirculation occurs in the center region for both entrance profiles.

The pressure rise in front of the cell is associated with the front stagnation point, the minimum pressure is associated with the maximum negative velocity, and the pressure rise that follows is associated with the rear stagnation point. The pressure distribution for plug profile as a function of velocity ratio is shown in Fig. 8. At low velocity ratios the mixture viscosity is no longer close to the viscosity of the outer jet; hence the fully developed pressure gradient changes. The case of $w_2/w_1 = 1$ demonstrates this quite clearly. When the velocity ratio is smaller than unity, the inner jet is faster and acts as a jet pump. Initially, there is a pressure decrease; farther downstream the pressure rises; and finally the confining wall influences the flow development and the pressure decreases until fully developed conditions are reached (not shown here). The cells formed for the case of a faster moving inner jet are situated along the confining wall and are much longer than in the case of a fast moving outer jet.

Experimental Results

The first objective in the experimental study was to establish the steady laminar regime of homogeneous and heterogeneous jet mixing. Hot-wire anemometery (outputs displayed on an oscilloscope), was used to obtain the local behavior of the

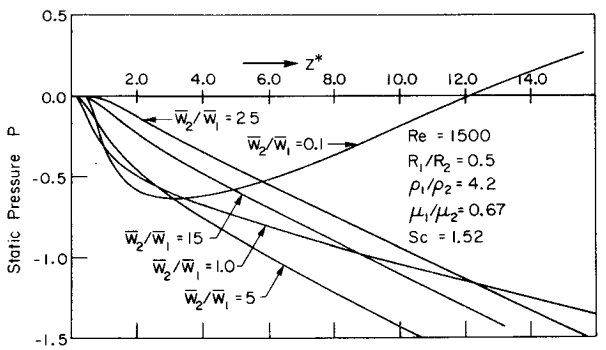

Fig. 8 Pressure development along centerline.

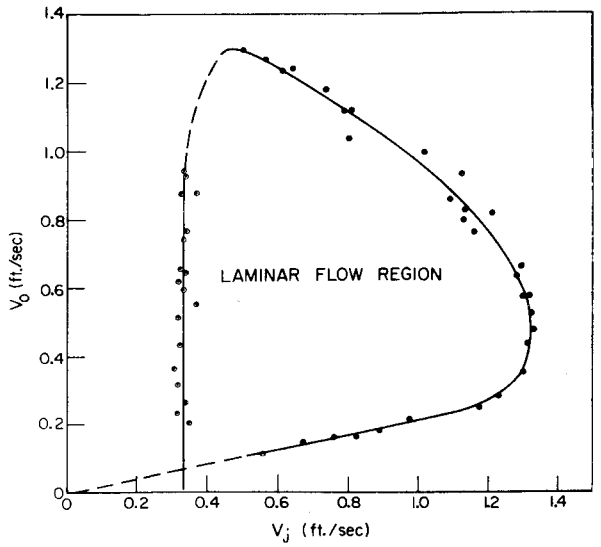

Fig. 9 Laminar region for air-argon system.

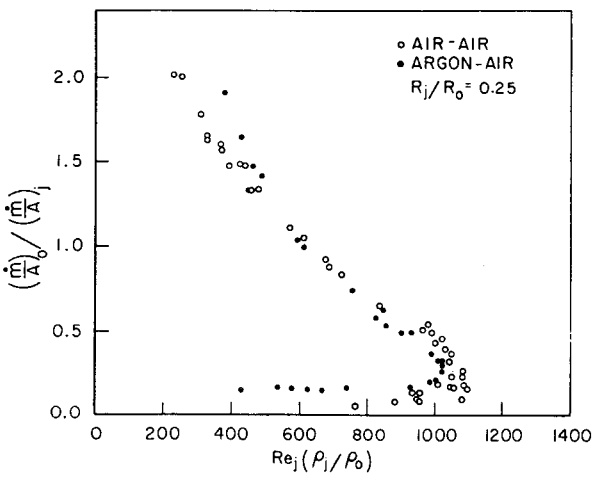

Fig. 10 Mass flux vs jet Reynolds number.

mixture at given velocity ratios. In addition, each individual jet was checked to see whether the approaching flow was steady and laminar.

The laminar flow region for heterogeneous jet mixing (argon-air) is shown in Fig. 9. The circled data indicates the conditions under which the flow just ceased to appear steady and laminar. The continuous line is the best fit (determined by visual observation) that established the boundary of the laminar flow region. The broken lines are an extrapolation of the laminar region boundary. The density ratio of argon and air is 1.37. Argon, the heavy gas, flows in the inner tube; air flows in the annular tube. The regime for heterogeneous jets, shown in Fig. 10, extends up to an inner jet velocity of 1.34 fps and an outer jet velocity of 1.3 fps. For inner velocities smaller than 0.33 fps the flow is unstable for all outer jet velocities. For inner jet velocities greater than 0.33 fps, these instabilities disappear.

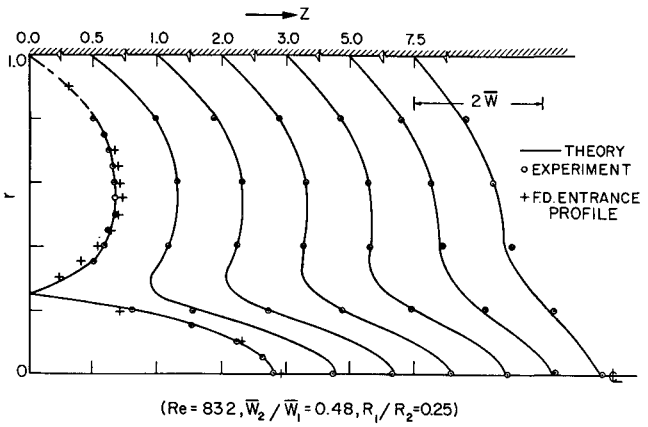

Fig. 11 Axial velocity profiles.

The laminar flow region for homogeneous jet mixing is found to be much larger. The region extends up to inner jet velocity of 2.26 fps and an outer jet velocity of 1.34 fps. Plotting the homogeneous and heterogeneous data in terms of outer to inner jet mass flux ratio vs the Reynolds number of the inner jet multiplied by the density ratio (ρ_j/ρ_0) collapses the data into a single curve; see Fig. 10. The maximum value of $R_{ej}(\rho_j/\rho_0)$ for which the flow remains laminar is approximately 1060. The instabilities in the heterogeneous case, for $R_{ej}(\rho_j/\rho_0) < 245$ are believed to be due to gravitational effects.

The measurements of the hydrodynamic development of the homogeneous jets (air-air) at laminar flow conditions are shown in Fig. 11. The dots represent the measured data, and the solid lines represent the calculated velocity profiles. The only measured information used in the calculations are the entrance conditions. The plus signs in Fig. 11 represent the fully developed profile for the given flow condition, which does not coincide with the actual measured profile.

The measurement of the concentration profiles for the heterogeneous jets (argon-air) is shown in Fig. 12. The velocity ratio

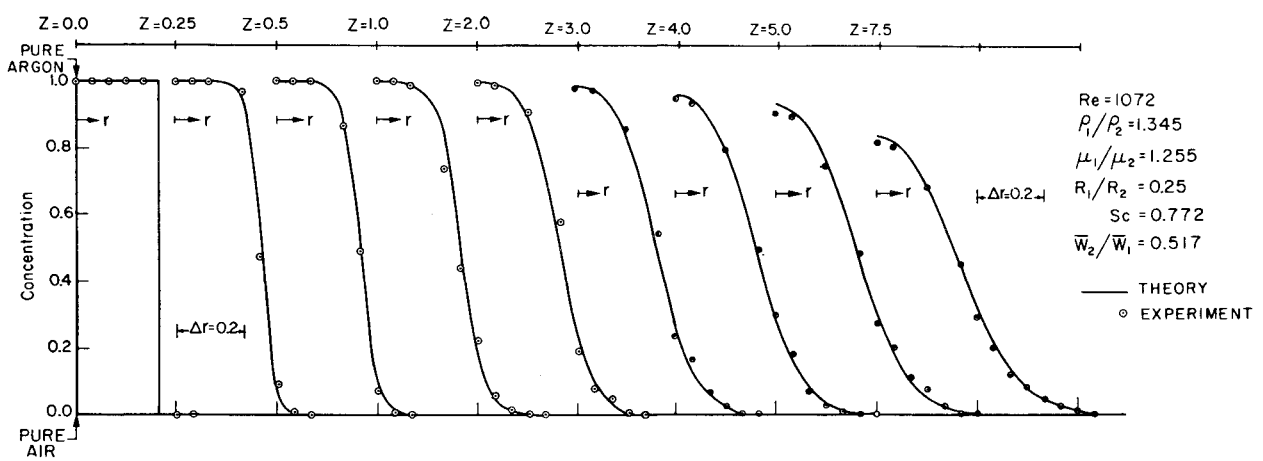

Fig. 12 Concentration profiles.

selected falls in the region of laminar flow. Again the dots represent the measured values and the solid lines represent the numerical calculations based on the measured velocity profile at the entrance to the mixing section (it is possible to measure the velocity profile of each individual, unmixed stream at the entrance to the mixing region with the hot wire). The largest deviation between the calculated and measured values occurs at the sharp concentration gradients in the interface, where the finite size of the aspirating probe may introduce errors.

Conclusion

The velocity profiles prescribed upstream of the entrance to the mixing region are the correct boundary condition for mixing of confined jets, since they allow an upstream influence. All results based on velocity profiles prescribed at the entrance to the mixing region represent at best a situation where the entrance velocity profiles are generated artificially. Cell formation takes place when inner jet momentum is much smaller than the momentum of the outer jet. For given parameters the cell grows upstream as velocity ratio increases, while its downstream end hardly moves. When the plug profiles are used as the entrance boundary condition at $z = 0$, they generate recirculating cells at higher velocity ratios than the fully developed profiles.

The regime of steady laminar flow of homogeneous (air-air) and heterogeneous (argon-air) jet mixing in a confining tube of radius ratio 0.25 (0.5 in./2.0 in.) was established. The regime for heterogeneous jets (argon-air) was found to be much smaller. The parameter correlating the stability of the homogeneous and heterogeneous laminar regions is the density ratio of the pure components. The measurements of the hydrodynamic development of the homogeneous jets and the concentration profiles for heterogeneous jets agree very well with the numerical solutions when the measured velocity profiles at the entrance to the mixing region is used as a boundary condition.

References

[1] von Kármán, T., "Theoretical Remarks or Thrust Augmentation," *Reissner Anniversary Volume*, University of Michigan Publication, Ann Arbor, 1949.

[2] Weinstein, H. and Todd, C. A., "A Numerical Solution of the Problem of Mixing of Laminar Coaxial Streams of Greatly Different Densities—Inothermal Case," TND-1534, Feb. 1963, NASA.

[3] Wood, B., "Diffusion in Laminar Confined Jet," D.Sc. thesis, 1964, Chemical Engineering Dept., MIT, Cambridge, Mass.

[4] Seider, W. D. and Churchill, S. W., "Confined Jet Mixing in the Entrance of a Tubular Reactor," *AICHE Journal*, Vol. 17, No. 3, May 1971, pp. 704–712.

[5] Ghia, K. M., Torda, T. P., and Lavan, Z., "Laminar Mixing of Heterogeneous Axisymmetric Coaxial Confined Jets," *AIAA Journal*, Vol. 7, No. 11, Nov. 1969, pp. 2072–2078.

[6] Shavit, G., "Analytical and Experimental Investigation of Laminar Mixing of Homogeneous and Heterogeneous Jets in a Confining Tube," Ph.D. thesis, June 1970, Mechanical Engineering Dept., Illinois Inst. of Technology.

[7] Ruddenberg, J. W. and Wilke, C. R., "Calculation of the Mixture Viscosities," *Industrial and Engineering Chemistry Journal*, Vol. 41, No. 7, July 1949.

[8] Chapman, S. and Cowling, T. C., *The Mathematical Theory of Non-Uniform Cases*, Cambridge University Press, New York, 1939.

[9] Reid, R. C. and Sherwood, T. R., *The Properties of Gases and Liquids*, McGraw-Hill, New York, 1966.

[10] Lavan, Z., "Investigation of Swirling Flow in Ducts," Ph.D. thesis, 1965, Mechanical Engineering Dept., Illinois Inst. of Technology.